

RESEARCH ARTICLE

Comparison of linear measurements between CBCT orthogonally synthesized cephalograms and conventional cephalograms

¹S Yang, ²D G Liu and ¹Y Gu

¹Department of Orthodontics, Peking University School and Hospital of Stomatology, Beijing, China; ²Department of Oral Radiology, Peking University School and Hospital of Stomatology, Beijing, China

Objectives: The purposes of the study are to investigate the consistency of linear measurements between CBCT orthogonally synthesized cephalograms and conventional cephalograms and to evaluate the influence of different magnifications on these comparisons based on a simulation algorithm.

Methods: Conventional cephalograms and CBCT scans were taken on 12 dry skulls with spherical metal markers. Orthogonally synthesized cephalograms were created from CBCT data. Linear parameters on both cephalograms were measured via Photoshop CS v. 5.0 (Adobe® Systems, San Jose, CA), named measurement group (MG). Bland–Altman analysis was utilized to assess the agreement of two imaging modalities. Reproducibility was investigated using paired *t*-test. By a specific mathematical programme “cepha”, corresponding linear parameters [mandibular corpus length (Go-Me), mandibular ramus length (Co-Go), posterior facial height (Go-S)] on these two types of cephalograms were calculated, named simulation group (SG). Bland–Altman analysis was used to assess the agreement between MG and SG. Simulated linear measurements with varying magnifications were generated based on “cepha” as well. Bland–Altman analysis was used to assess the agreement of simulated measurements between two modalities.

Results: Bland–Altman analysis suggested the agreement between measurements on conventional cephalograms and orthogonally synthesized cephalograms, with a mean bias of 0.47 mm. Comparison between MG and SG showed that the difference did not reach clinical significance. The consistency between simulated measurements of both modalities with four different magnifications was demonstrated.

Conclusions: Normative data of conventional cephalograms could be used for CBCT orthogonally synthesized cephalograms during this transitional period.

Dentomaxillofacial Radiology (2014) **43**, 20140024. doi: [10.1259/dmfr.20140024](https://doi.org/10.1259/dmfr.20140024)

Cite this article as: Yang S, Liu DG, Gu Y. Comparison of linear measurements between CBCT orthogonally synthesized cephalograms and conventional cephalograms. *Dentomaxillofac Radiol* 2014; **43**: 20140024.

Keywords: Cone beam computed tomography; orthodontics; measurement

Introduction

With the development of CT technology, CBCT is becoming a promising modality to analyse malocclusions and to evaluate the effects of orthodontic, orthopaedic and surgical interventions etc. In particular, CBCT images enable us to perform a three-dimensional (3D) assessment

of the craniofacial complex in life size without distortion or overlapping of anatomical structures.^{1–7}

Longitudinal two-dimensional (2D) cephalometric records contain tables and graphs with average values of linear dimensions and angles, computed at yearly intervals for males and females separately. These records facilitate our understanding of the maxillofacial growth curve, which is crucial for diagnosis and treatment

Correspondence to: Dr Yan Gu. E-mail: guyan99@gmail.com

Received 19 January 2014; revised 10 July 2014; accepted 15 July 2014

Table 1 Landmarks used in the study

Point	Description
1. Nasion (N)	The most anterior median point on the frontonasal suture
2. A point (A)	The most posterior median point on the concavity of the contour of the premaxilla between the anterior nasal spine and the crest of the maxillary alveolar process
3. Anterior nasal spine (ANS)	The most anterior median point on the anterior nasal spine
4. Gnathion (Gn)	The most inferior and anterior point on the midline of the bony chin
5. Menton (Me)	The most inferior point on the midline of the bony chin
6. Orbitale right (OrR)	The most inferior point on the inferior margin of the right orbit
7. Orbitale left (OrL)	The most inferior point on the inferior margin of the left orbit
8. Porion right (PoR)	The most superior lateral point of the right external auditory meatus
9. Porion left (PoL)	The most superior lateral point of the left external auditory meatus
10. Condyle right (CoR)	The most superior posterior median point of the right condylar head
11. Condyle left (CoL)	The most superior posterior median point of the left condylar head
12. Gonion right (GoR)	The midpoint on the curvature of the angle of the mandible where the ramus and the body of the mandible meet on the right side
13. Gonion left (GoL)	The midpoint on the curvature of the angle of the mandible where the ramus and the body of the mandible meet on the left side
14. Sella (S)	The median point of the bottom of pituitary fossa ^a

^aThe location of sella was altered for landmark labelling.

evaluation of skeletal malocclusion. However, a few studies stated that direct comparison of 2D and 3D cephalometry was infeasible.^{6,8,9} Gribel *et al*⁶ stressed that 2D cephalometric norms could not be readily used for 3D measurements. Van Vlijmen *et al*⁸ recommended that 3D tracings were not suitable for longitudinal research in cases where there were only 2D records from the past. Some investigators advocated the use of synthesized cephalometric images from CBCT as the bridge for the analysis in the transitional period from 2D to 3D.^{10–18}

There are two fundamental projection methods to create 2D images from CBCT data: orthogonal projection and perspective projection.¹¹ Orthogonal projection has a centre of projection (focus) at an infinite distance from the plane of projection, thus simulating parallel rays, whereas perspective projection sets the focus at a finite distance from the plane of projection, simulating the geometry of the conventional cephalometric radiographs. The source-to-object and object-to-film distances should be set identically to specific cephalometer distances when constructing perspective

synthesized cephalograms from CBCT data volume via software.¹⁴ Furthermore, Lamichane *et al*¹⁴ claimed that perspective lateral images from CBCT data could replicate the inherent magnification of conventional 2D lateral cephalograms with high accuracy, and they could be used in comparison with 2D normative data or serial records.

In previous studies, Dibbets explored the effect of radiographic magnification in linear dimensions from five major longitudinal cephalometric databases.^{19,20} He mentioned that some vital data on focus-radiograph and midsagittal-radiograph distances were lacking,²⁰ which are indispensable parameters for generating perspective synthesized cephalograms from CBCT data as confirmed.¹⁴ To fully utilize 2D normative values during this transitional period, we might need to turn our attention to investigate the compatibility in the measurements between conventional cephalograms and orthogonally synthesized cephalograms, since reconstruction algorithm of the latter from CBCT data is simpler, with no need for distance setting.

The existing evidence proved that there was no statistically or clinically relevant difference between these two types of cephalograms on angles or distances, such as upper anterior facial height (N-ANS), lower anterior facial height (ANS-Me) and facial height (NMe), after corrected by midsagittal magnification.^{12,13,15} However, comparison regarding common linear measurements in longitudinal research, such as mandibular corpus length (Go-Me), mandibular ramus height (Co-Go) and posterior facial height (Go-S), was less involved in previous investigations. The related landmarks were located at different sagittal planes, leading to disproportionate enlargement distortion on the traditional lateral radiographs,^{6,21} and the amount of distortion was determined by the respective focus-radiograph and midsagittal-radiograph distances. The study by Oz *et al*¹⁶ showed that linear measurement (Go-Me) differed significantly between conventional cephalograms and orthogonally

Table 2 Linear measurements used in the study^a

Linear measurement	Description
N-ANS	Nasion to anterior nasal spine A. Represents anterior upper facial height
ANS-Me	Anterior nasal spine to menton. Represents anterior lower face height
Co-A	Condylion to point A. Represents midfacial length
Co-Gn	Condylion to gnathion. Represents mandibular length
Go-Me	Gonion to menton. Represents mandibular body length
Co-Go	Gonion to condylion. Represents mandibular ramus height
Go-S	Gonion to sella. Represents posterior facial height

^aBilateral values of Co-A, Co-Gn, Go-Me, Co-Go, Go-S derived from left, right synthesized cephalograms were divided equally.



Figure 1 Measurements on the conventional cephalometric radiograph via Photoshop CS (Adobe® Systems, San Jose, CA).

synthesized cephalograms. He explained this might be owing to greater margins of error in the identification of the landmarks Go and Me. It could be assumed that the potential confounding factors, head orientation or landmark identification,²² might interfere with our judgment about the inherent difference of linear parameters between the two modalities. Additionally, we noticed that normative data of conventional cephalograms were

derived from longitudinal research with various magnifications, but few studies explored if different magnifications could affect the comparison between conventional cephalograms and orthogonally synthesized cephalograms. Therefore, in the present study, a mathematical simulation was generated for the comparison of measurements between them at various magnifications, by which multiple landmark localization and head orientation on both cephalograms could be well controlled. Above all, the purpose of this study was to investigate the consistency of linear measurements between orthogonally synthesized cephalograms from CBCT and conventional cephalograms. The article is focused on two parts: (1) to compare linear measurements of the related landmarks located on different sagittal planes between conventional cephalograms and orthogonally synthesized cephalograms and (2) to explore the influence of different magnification on the comparisons.

Methods and materials

Specimen preparation

The sample consisted of 12 undocumented dry skulls obtained from the collection of the Department of Anatomy (Peking University Health Science Center, Beijing, China). The criterion for inclusion was as follows: the skulls and mandibles were well preserved without visible asymmetry. The mandible was matched with the skull, based on midline coincidence and the position of the condyles in the fossa. The mandibular position was fixed with wax plate between jaws and broad tape from the ipsilateral temporal bone around the inferior border of the mandibular body to the contralateral temporal

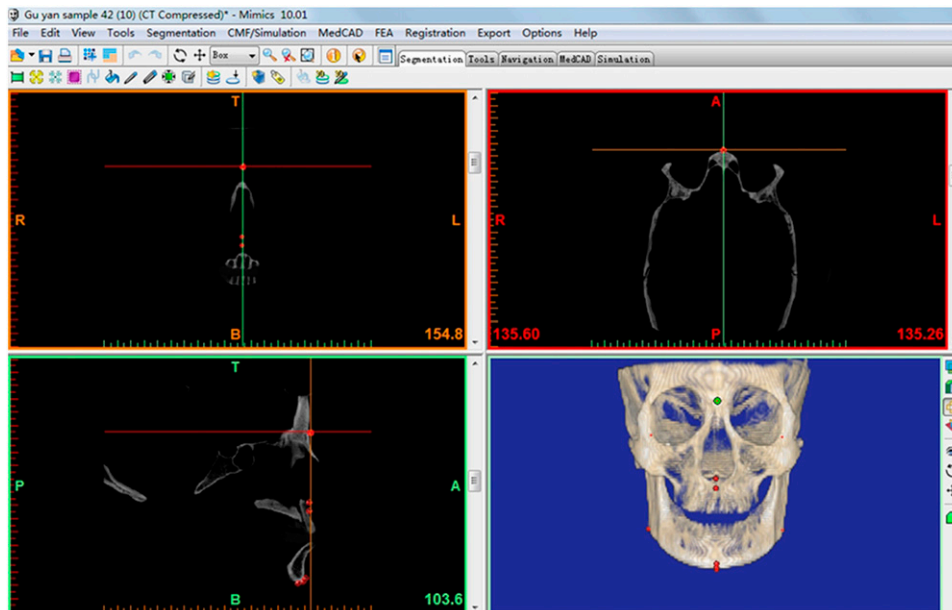


Figure 2 Landmark identification on the axial, coronal and sagittal slices in Mimics® (Materialize Co., Leven, Belgium). A, anterior; B, bottom; L, left; P, posterior; R, right; T, top.

bone. The skulls were number coded to allow identification of each specimen. Spherical metal markers (1 mm in diameter) were glued on 14 selected landmarks according to their descriptions (Table 1).

Radiography

Each skull was positioned in the cephalostat (ORTHOCEPH[®] OC200; Instrumentarium Corp., Graven, Finland; 77 kVp; 16 mAs; 0.16 s) by fixing it between the ear rods. A custom foam platform was employed to support the skulls during imaging, and the Frankfurt horizontal plane was parallel to the floor. The magnification of the particular machine used in this study was 1.144 for all subjects. The distance from X-ray source to midline of the object was 152.3 cm and that of film to midline of the object was 22 cm.

Each specimen was scanned by DCT Pro[®] (Vatech, Co., Ltd, Yongin-Si, Republic of Korea) operated at 75 kV and 6.5 mAs. With the custom foam platform, skulls were oriented to the Frankfort horizontal plane parallel to the floor and the midsagittal plane perpendicular to the floor. Left, right orthogonally synthesized cephalograms were created from CBCT.

Identification and comparison of seven linear measurements:

Seven linear parameters (Table 2) on conventional cephalograms and orthogonally synthesized cephalograms were measured via Photoshop CS v. 5.0 (Adobe[®] Systems, San Jose, CA) (Figure 1). In this study, the centre of metal markers was regarded as the location of the related landmarks. As for bilateral structures, the distance between the centres of the two bilateral metal markers was divided in two to determine where the cephalometric landmark could be located. Values obtained from orthogonally synthesized cephalograms were adjusted for the 14.4% magnification of the cephalostat. The same operator performed the landmark identification and digital measurements two times, with an interval of 3 weeks.

Analysis of the data was conducted with MedCalc[®] (Mariakerke, Belgium). Bland–Altman analysis was utilized to assess the agreement of linear measurements from the two modalities. Reproducibility of the operator's measurement was investigated using paired *t*-tests.

Simulation algorithm of linear measurements: The CBCT axial images were exported in digital imaging and communications in medicine format and imported

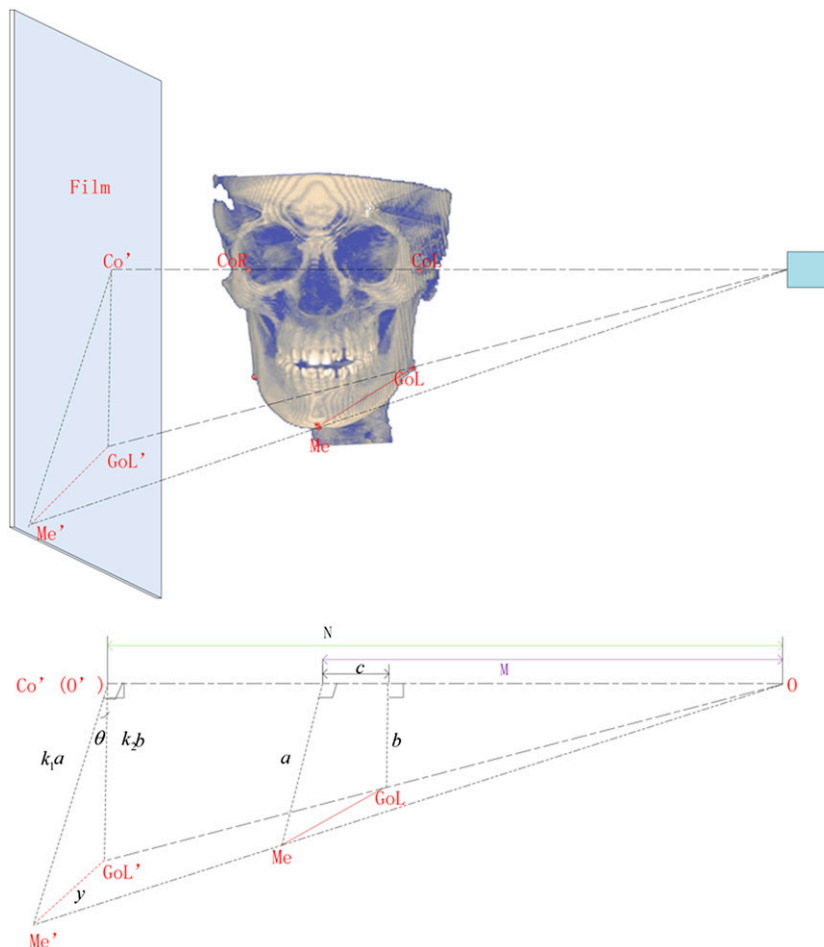


Figure 3 Illustration of algorithm applied on gonion left–menton (GoL–Me) on the conventional cephalogram.

into software (Mimics® v. 10.01; Materialize Co., Leuven, Belgium). In Mimics, the centres of metal markers were identified by a cursor-driven mouse on the axial, coronal and sagittal slices to obtain co-ordinates of related landmarks (Figure 2). Based on respective imaging principles and trigonometric functions, a mathematical programme “cepha” was made using MATLAB® (MathWorks®, Natick, MA) to obtain simulated values of linear measurements (Go-Me, Co-Go, Go-S).

The algorithm is illustrated as follows:

1. Simulation of linear measurements (Go-Me, Go-S) on conventional lateral cephalograms.

Both landmarks (Me, S) are on the midsagittal plane, therefore, Go-Me, Go-S are distorted or magnified in the same manner. Take GoL-Me, for example (Figure 3). The formula is:

$$y = \sqrt{(k_1 a)^2 + (k_2 b)^2 - 2 \cdot (k_1 a) \cdot (k_2 b) \cdot \cos \theta}$$

OO': central line of X-ray (CoR-CoL)

a: distance from point Me to central line of X-ray beam (CoR-CoL)

b: distance from point GoL to central line of X-ray beam (CoR-CoL)

c: distance between line a and line b

θ : angle between line a and line b

y: linear value on the conventional lateral head film

k_1 : magnification factor at the midsagittal plane of a skull

k_2 : magnification factor at the sagittal section passing through related landmark GoL.

By definition, k_2_GoL = distance from X-ray source to film/distance from X-ray source to the sagittal section passing through GoL.

2. Simulation of linear measurements Co-Go on conventional lateral cephalograms.

Take GoL-CoL, for example (Figure 4). Since the effects of magnification are negligible at CoL, the formula is simplified as $y = k_2 b$

b: distance from point GoL to central line of X-ray beam (CoR-CoL)

y: linear value on the conventional lateral head film.

3. Simulation of linear measurements (Go-Me, Go-S, Co-Go) on orthogonally synthesized cephalograms from CBCT.

Take GoL-Me, GoL-CoL, for example (Figure 5). The formula is $y = a \cos \theta$

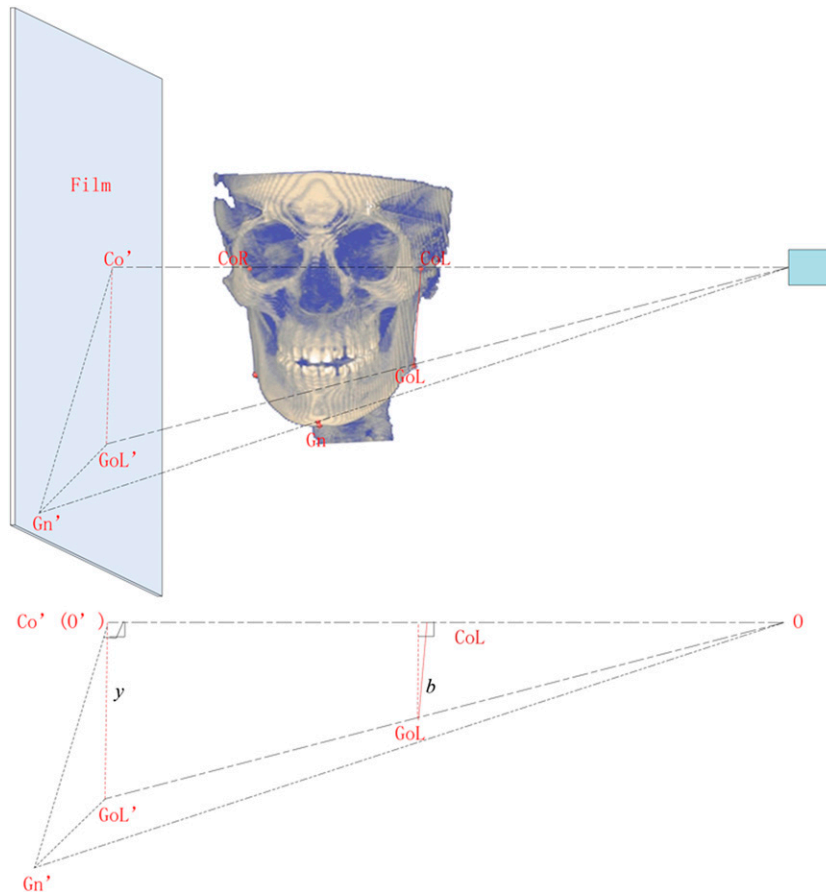


Figure 4 Illustration of algorithm applied on condyle left-gonion left (CoL-GoL) on the conventional cephalogram.

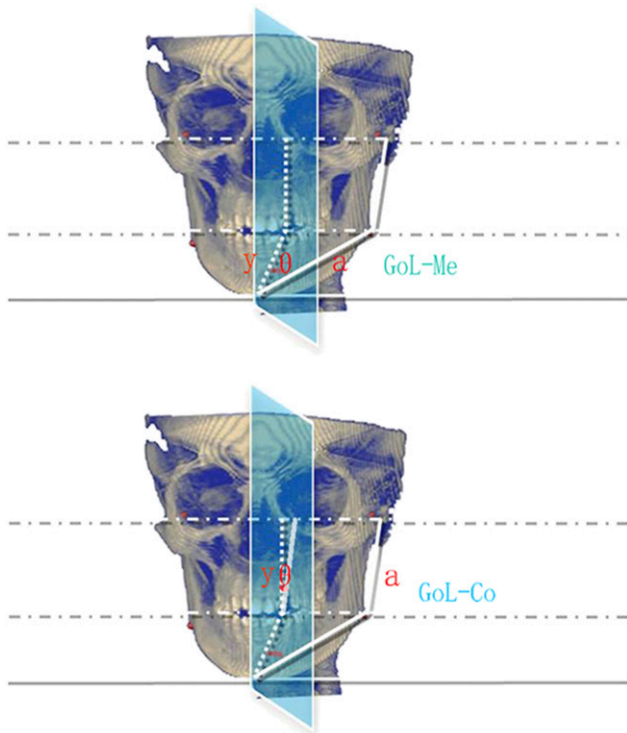


Figure 5 Illustration of algorithm applied on gonion left–menton (GoL–Me) and condyle left–gonion left (CoL–GoL) on the orthogonally synthesized cephalogram.

a : 3D dimensions of GoL–Me or GoL–Co

θ : angle between GoL–Me and the midsagittal plane or angle between GoL–CoL and the midsagittal plane

y : linear value on the orthogonally synthesized cephalogram.

After co-ordinates and specific focus–radiograph and midsagittal–radiograph distances of the machine we used were input, values of k_1 and k_2 , a and b , c and θ mentioned above were automatically calculated by the given programme “cepha”. Subsequently, corresponding linear parameters (Go–Me, Co–Go, Go–S) of these two types of cephalograms were exported, named simulation group (SG), whereas the previous measurements of each kind via Photoshop CS v. 5.0 were named measurement group (MG).

Simulated linear measurements (Go–Me, Co–Go, Go–S) of conventional cephalograms with four varying magnifications were generated based on “cepha” as well. Respective X–ray source–midsagittal and midsagittal–radiograph distances were gathered from the previous literature (Table 3).^{11,14,23} Simulated linear values of orthogonally synthesized cephalograms were corrected by

Table 3 Distances of X–ray source midsagittal and midsagittal radiograph at four common magnifications (cm)

Distance	Midsagittal magnification			
	7.5%	10%	12.5%	14.4%
X–ray source–midsagittal plane	152.4	150.0	144.0	152.3
Midsagittal plane–radiograph	11.5	15.0	18.0	22.0

the corresponding midsagittal magnification. Bland–Altman analysis was utilized to assess the agreement of simulated measurements between the two modalities.

Results

No statistically significant difference was noted between repeated measurements on both kinds of cephalograms (Table 4, $p > 0.05$). Descriptive statistics for each measurement is shown in Table 5. Bland–Altman analysis revealed the agreement between measurements on conventional cephalograms and orthogonally synthesized cephalograms, with a mean bias of 0.47 mm [95% limits of agreement (LOA): -0.31 to 1.25 mm] (Figure 6). Hence, it could be considered that there was no clinically relevant difference between them.

Comparisons between MG and SG of both modalities were depicted in Table 6. Bland–Altman plots demonstrated excellent agreement between MG and SG of each type, with a mean difference of 0.17 mm (95% LOA: -0.75 – 1.10 mm) for conventional cephalograms and a mean difference of -0.16 mm (95% LOA: -1.14 – 0.83 mm) for orthogonally synthesized cephalograms, verifying the accuracy of the simulation algorithm we developed (Figures 7 and 8).

Descriptive statistics of simulated measurements is respective magnification were shown in Table 7. Mean bias and LOA in Bland–Altman analysis for each assessment is summarised in Table 8. The consistency between simulated measurements of both modalities with four different magnifications was demonstrated.

Discussion

Considering notable difference between 2D and 3D images, many researchers tried to figure out whether CBCT synthesized cephalograms could be used to take the place of traditional lateral radiographs. A finding presented that the measurements of 17 angles from Bjork analysis did not differ between conventional lateral cephalograms and synthesized cephalograms in 34 patients.¹² The study by Van Vlijmen *et al*,¹⁵ using

Table 4 Paired t -test for repeated measurements on both modalities

Modality	Mean	Standard deviation	p-value
Conventional cephalogram	0.019	0.148	0.253
CBCT orthogonally synthesized cephalogram	0.092	0.926	0.235

Table 5 Mean values and standard deviation (SD) for each measurement on both cephalograms (mm)

Measurement	Conventional cephalogram		Orthogonally synthesized cephalogram		Difference	
	Mean	SD	Mean	SD	Mean	SD
N-ANS	59.246	4.694	58.629	4.610	0.617	0.142
ANS-Me	69.638	6.048	69.316	6.227	0.322	0.434
Co-A	92.816	5.284	92.197	4.925	0.618	0.493
Co-Gn	124.801	5.117	124.195	5.076	0.606	0.293
Go-Me	75.587	3.095	75.426	3.147	0.161	0.410
Co-Go	68.325	5.490	67.851	5.506	0.474	0.394
Go-S	83.985	6.093	83.521	6.005	0.464	0.373

A, a point; ANS, anterior nasal spine; Co, condyle; Diff, difference; Gn, gnathion; Go, gonion; Me, menton; N, nasion; S, sella.

40 dry skulls, stated that the average difference for these measurements (SNB, NSL/NL, NL/ML, ILs/NL, ILi/ML and interincisal angle) between both modalities was statistically significant, whereas the actual mean average difference ranged from -1.54° to 1.45° , similar to or smaller than the standard error for the repeated measurements. Therefore, the author stressed that the difference did not reach clinical significance. Overall, it is accepted that CBCT orthogonally synthesized cephalograms can successfully replace conventional lateral films in angular measurements.¹⁵

As mentioned earlier, orthogonal and perspective projection are two fundamental projection methods to create 2D images from CBCT data.¹¹ Since there is no need for distance setting, constructing 2D lateral images from CBCT data by orthogonal projection would be preferred, and this makes it possible for the comparison with the previous 2D serial records, when some vital data on focus-radiograph and midsagittal-radiograph distances were lacking.²⁰

Common linear measurements from longitudinal research could be grouped into three types, according to their related reference landmarks.

In Type 1, two landmarks are both located on the midsagittal plane, such as N-ANS, ANS-Me

Linear dimensions of this type are enlarged uniformly on conventional cephalograms by the magnification of the particular machine, whereas no enlargement exists on orthogonally synthesized cephalograms (Figure 9). Some researchers suggested that the distances of this type were comparable between them, after adjustment by the specific magnification.^{13,16}

In Type 2, one landmark is on the midsagittal plane and the other is Co, such as Co-A, Co-Gn

Linear dimensions of this type, occupying different sagittal planes, present with distortion to different extents on the two imaging modalities. The distortion on the conventional cephalogram is essentially disproportionate enlargement of the given structure.²¹ With reference to Figure 10, the X-ray central beam is perpendicular to the midsagittal plane and passing through CoR and CoL, where the magnification effects are negligible. In the light of trigonometric functions, the values of Co-A, Co-Gn on the conventional cephalogram equal the projection of each 3D measurement on the midsagittal plane multiplying the midsagittal magnification. Based on this principle, Gribel *et al*⁶ rectified the measurements made on conventional lateral films to corresponding dimensions observed in CBCT scans in human subjects.

As for CBCT orthogonally synthesized cephalograms, the virtual parallel beam is also perpendicular to the midsagittal plane (Figure 10). Thus, its values of Co-A, Co-Gn equal the projection of each 3D measurement on the midsagittal plane.⁶ It was found that the distances of this type were comparable between them as well, after adjustment by the specific magnification. Generally, these comparative results of both Types 1 and 2 are consistent with those of our study.^{13,15}

In Type 3, one landmark is on the midsagittal plane or Co and the other is Go, such as Go-Me, Co-Go, Go-S

Similar to Type 2, linear dimensions of Type 3 also transverse different sagittal planes (Figure 11). The projection of related 3D measurements on the midsagittal plane—"d2" still represents its value on the orthogonally synthesized cephalogram. However, the magnification of the sagittal plane through Go is not

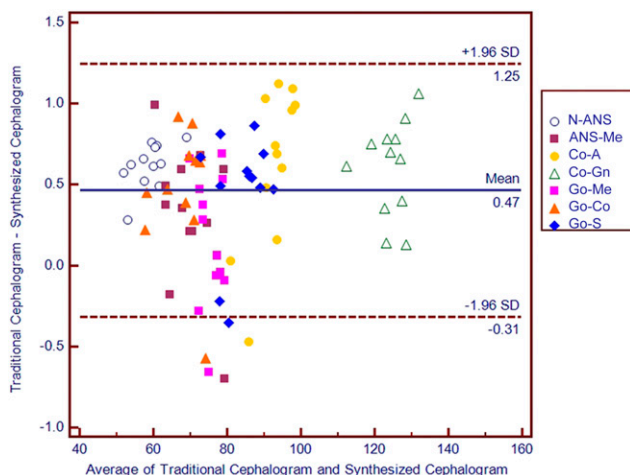


Figure 6 Bland-Altman analysis between measurements on conventional cephalograms and orthogonally synthesized cephalograms. A, a point; ANS, anterior nasal spine; Co, condyle; Gn, gnathion; Go, gonion; Me, menton; N, nasion; S, sella; SD, standard deviation.

Table 6 Comparisons between measurement group (MG) and simulation group (SG) of both modalities (mm)

Modality	Measurement	MG		SG		Difference	
		Mean	SD	Mean	SD	Mean	SD
Conventional cephalogram	Go-Me	75.587	3.095	75.603	3.142	-0.016	0.305
	Co-Go	68.325	5.490	68.393	5.625	-0.068	0.404
	Go-S	83.985	6.093	83.383	6.060	0.602	0.384
Orthogonally synthesized cephalogram	Go-Me	75.426	3.147	75.631	3.174	-0.206	0.483
	Co-Go	67.851	5.506	68.313	5.595	-0.462	0.306
	Go-S	83.521	6.005	83.322	6.037	0.199	0.489

Co, condyle; Diff, difference; Go, gonion; Me, menton; S, sella; SD, standard deviation.

clear, so the distortion of related linear dimensions on conventional cephalometric image—“d1” is more complicated than that of Type 2 and not easily qualified. For one subject, “d2” is settled while “d1” varies according to different focus-radiograph and midsagittal-radiograph distances. So far, comparative studies between the two imaging modalities involved little about linear measurements of this type, while these measurements represent the magnitude and direction of mandibular growth.¹⁹

In this study, mean differences of Go-Me, Co-Go, Go-S between CBCT orthogonally synthesized cephalograms and conventional cephalograms ranges from 0.161 to 0.474 mm, which means “d1” closely approximated midsagittal magnification multiplying “d2”. However, it was reported that linear measurement (Go-Me) differed significantly between these two cephalograms, and the absolute mean difference was -2.245 mm.¹⁶ One possible explanation for this disparity was that we used spherical metal fiducials to enhance the accuracy of landmark identification and subsequent linear measurements. Moreover, the magnification of the cephalostat was set at 1.125 in the study by Oz *et al*¹⁶ but 1.144 in ours.

Linear measurements of all types on both cephalograms were well matched in our study. However, as for

Type 3, it is not explicit whether the difference between them could be reliably compensated by midsagittal magnification once cephalometric geometry changed. That is why we established the simulation programme “cepha” in order to facilitate comparison of linear dimensions at various magnifications. The excellent agreement between MG and SG proved the reliability of this simulation algorithm (Table 6, Figures 7 and 8). Although the difference of projection distortion in linear measurement (Go-Me, Co-Go, Go-S) between these two types of cephalograms could be hypothesized, as we discussed before, this study showed that simulated measurements of Go-Me, Co-Go, Go-S were comparable with various magnifications.

In the present study, the selected specimen had no visible asymmetry, and every skull’s position was carefully orientated when radiographic images were taken. All of these contributed to the perpendicularity of the X-ray central beam OO’ or virtual parallel beam to the midsagittal plane of skulls, and such traits of head orientation were made default settings in the programme “cepha”. Also, landmarks were located in multiplanar reformatted images, which had been recommended to improve the accuracy of landmark selection^{24–26} and labelled with metal markers, so we could obtain more reliable co-ordinates of corresponding landmarks in

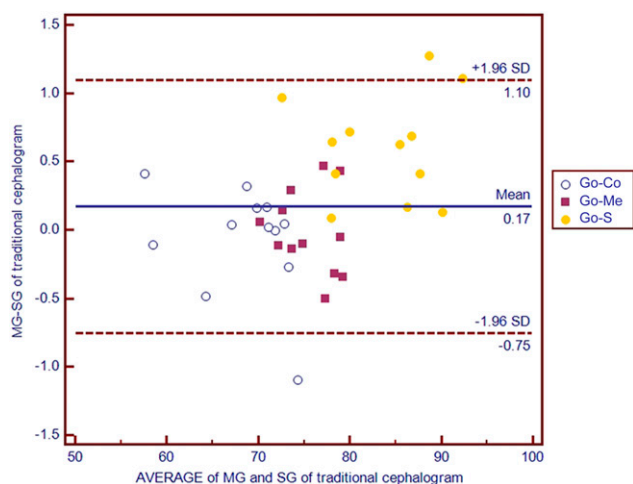


Figure 7 Bland–Altman analysis between measurement group (MG) and simulation group (SG) of conventional cephalograms. Co, condyle; Go, gonion; S, sella; SD, standard deviation.

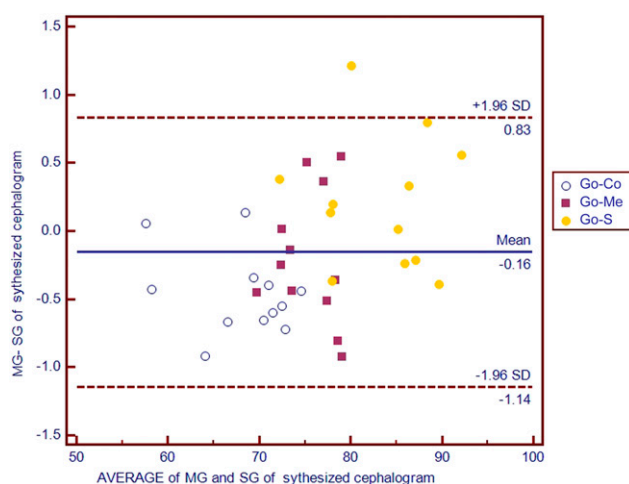


Figure 8 Bland–Altman analysis between measurement group (MG) and simulation group (SG) of orthogonally synthesized cephalograms. Co, condyle; Go, gonion; S, sella; SD, standard deviation.

Table 7 Descriptive statistics of simulated values with four magnifications (mm)

Magnification (%)	Measurement	Simulated values of conventional cephalogram		Simulated values of orthogonally synthesized cephalogram		Difference	
		Mean	SD	Mean	SD	Mean	SD
7.5	Go-Me	71.042	2.953	71.070	2.983	-0.028	0.074
	Co-Go	64.270	5.286	64.193	5.258	0.078	0.115
	Go-S	78.427	5.649	78.368	5.628	0.059	0.105
10.0	Go-Me	72.707	3.021	72.723	3.052	-0.015	0.078
	Co-Go	65.738	5.407	65.685	5.380	0.053	0.119
	Go-S	80.455	5.902	80.430	5.896	0.025	0.125
12.5	Go-Me	74.359	3.088	74.375	3.122	-0.017	0.083
	Co-Go	67.237	5.532	67.178	5.503	0.059	0.127
	Go-S	82.033	5.922	81.992	5.902	0.041	0.117
14.4	Go-Me	75.587	3.095	75.603	3.142	-0.016	0.305
	Co-Go	68.393	5.625	68.313	5.595	0.008	0.122
	Go-S	83.383	6.058	83.322	6.038	0.062	0.113

Co, condyle; Go, gonion; Me, menton; S, sella; SD, standard deviation.

Mimics. Possible variables, landmark identification error or head position, were controlled well by these means, which was beneficial to improving the accuracy of the algorithm.

Some landmarks on synthesized cephalograms from CBCT might be identified even more easily than those on conventional cephalograms, probably owing to better visualization. Recently, Chang *et al*²⁷ comprehensively analysed potential variables affecting landmark identification errors. He concluded that the overall landmark identification errors on the two modalities were comparable, whereas Ba (the point where the median sagittal plane of the skull intersects the lowest point on the anterior margin of the foramen magnum) was more reliable on the CBCT-derived cephalograms. The simulation process avoided multiple

landmark localization on orthogonally synthesized cephalograms and conventional cephalograms. The midsagittal plane of each CBCT volume was vertical to the X-ray central beam OO' or parallel beam by default, which meant that the variations of head orientation and landmark identification were minimized. But in the clinical situation, *in vivo*, soft-tissue attenuation, metallic artefacts or patient motion may negatively affect the image quality and subsequent operations.²⁸ Image acquisition and tracing landmarks should be carefully carried out so that our results could be readily extrapolated to clinical practice.

In conclusion, linear measurements on both CBCT orthogonally synthesized cephalograms and conventional cephalograms were in concordance. Difference on these two imaging modalities could be compensated by midsagittal magnification. Head orientation and landmark identification should be carefully monitored in clinical practice. It also indicates that there is no need to take additional conventional cephalograms once CBCT data have been acquired. Longitudinal data derived from conventional cephalograms could be considered as the source of the norms for orthogonally synthesized cephalograms from CBCT during this transitional period.

Table 8 Mean bias and 95% limits of agreement (LOAs) in Bland-Altman analysis of simulated measurements with four magnifications between modalities (mm)

Magnification (%)	Mean bias	LOA
7.5	0.04	-0.17 to 0.25
10.0	0.02	-0.19 to 0.24
12.5	0.02	-0.20 to 0.25
14.4	0.04	-0.19 to 0.26

References

- Mozzo P, Procacci C, Tacconi A, Martini PT, Andreis IA. A new volumetric CT machine for dental imaging based on the cone-beam technique: preliminary results. *Eur Radiol* 1998; **8**: 1558-64.
- Hilgers ML, Scarfe WC, Scheetz JP, Farman AG. Accuracy of linear temporomandibular joint measurements with cone beam computed tomography and digital cephalometric radiography. *Am J Orthod Dentofacial Orthop* 2005; **128**: 803-11.
- Berco M, Rigali PH Jr, Miner RM, DeLuca S, Anderson NK, Will LA. Accuracy and reliability of linear cephalometric measurements from cone-beam computed tomography scans of a dry human skull. *Am J Orthod Dentofacial Orthop* 2009; **136**: e1-9.
- Moreira CR, Sales MA, Lopes PM, Cavalcanti MG. Assessment of linear and angular measurements on three-dimensional cone-beam computed tomographic images. *Oral Surg Oral Med Oral Pathol Oral Radiol Endod* 2009; **108**: 430-6. doi: [10.1016/j.tripleo.2009.01.032](https://doi.org/10.1016/j.tripleo.2009.01.032)
- Hans MG, Valiathan M, Palomo JM. Cone beam computed tomography: a link with the past, a promise for the future. *Semin Orthod* 2011; **17**: 81-7.
- Gribel BF, Gribel MN, McNamara JA, Manzi FR. From 2D to 3D: an algorithm to derive normal values for 3-dimensional computerized assessment. *Angle Orthod* 2011; **81**: 3-10.
- Mah JK, Yi L, Huang RC, Choo H. Advanced applications of cone beam computed tomography in orthodontics. *Semin Orthod* 2011; **17**: 57-71.
- Van Vlijmen OJ, Maal T, Bergé SJ, Bronkhorst EM, Katsaros C, Kuijpers-Jagtman AM. A comparison between 2D and 3D cephalometry on CBCT scans of human skulls. *Int J Oral Maxillofac Surg* 2010; **39**: 156-60.

9. Yitschaky O, Redlich M, Abed Y, Faerman M, Casap N, Hiller N. Comparison of common hard tissue cephalometric measurements between computed tomography 3D reconstruction and conventional 2D cephalometric images. *Angle Orthod* 2011; **81**: 11–16.
10. Farman AG, Scarfe WC. Development of imaging selection criteria and procedures should precede cephalometric assessment with cone-beam computed tomography. *Am J Orthod Dentofacial Orthop* 2006; **130**: 257–65.
11. Kumar V, Ludlow JB, Mol A, Cevidanes L. Comparison of conventional and cone beam CT synthesized cephalograms. *Dentomaxillofac Radiol* 2007; **36**: 263–9. doi: [10.1259/dmfr/98032356](https://doi.org/10.1259/dmfr/98032356)
12. Cattaneo PM, Bloch CB, Calmar D, Hjortshøj M, Melsen B. Comparison between conventional and cone-beam computed tomography-generated cephalograms. *Am J Orthod Dentofacial Orthop* 2008; **134**: 798–802.
13. Kumar V, Ludlow J, Soares Cevidanes LH, Mol A. *In vivo* comparison of conventional and cone beam CT synthesized cephalograms. *Angle Orthod* 2008; **78**: 873–9. doi: [10.2319/082907-399.1](https://doi.org/10.2319/082907-399.1)
14. Lamichane M, Anderson NK, Rigali PH, Seldin EB, Will LA. Accuracy of reconstructed images from cone-beam computed tomography scans. *Am J Orthod Dentofacial Orthop* 2009; **136**: 156.e1–6. doi: [10.1016/j.ajodo.2009.04.006](https://doi.org/10.1016/j.ajodo.2009.04.006)
15. Van Vlijmen OJ, Bergé SJ, Swennen GR, Bronkhorst EM, Katsaros C, Kuijpers-Jagtman AM. Comparison of cephalometric radiographs obtained from cone-beam computed tomography scans and conventional radiographs. *J Oral Maxillofac Surg* 2009; **67**: 92–7. doi: [10.1016/j.joms.2008.04.025](https://doi.org/10.1016/j.joms.2008.04.025)
16. Oz U, Orhan K, Abe N. Comparison of linear and angular measurements using two-dimensional conventional methods and three-dimensional cone beam CT images reconstructed from a volumetric rendering program *in vivo*. *Dentomaxillofac Radiol* 2011; **40**: 492–500.
17. Liedke GS, Delamare EL, Vizzotto MB, da Silveira HL, Prietsch JR, Dutra V, et al. Comparative study between conventional and cone beam CT-synthesized half and total skull cephalograms. *Dentomaxillofac Radiol* 2012; **41**: 136–42.
18. Park CS, Park JK, Kim H, Han SS, Jeong HG, Park H. Comparison of conventional lateral cephalograms with corresponding CBCT radiographs. *Imaging Sci Dent* 2012; **42**: 201–5. doi: [10.5624/isd.2012.42.4.201](https://doi.org/10.5624/isd.2012.42.4.201)
19. Dibbets JM, Nolte K. Comparison of linear cephalometric dimensions in Americans of European descent (Ann Arbor, Cleveland, Philadelphia) and Americans of African descent (Nashville). *Angle Orthod* 2002; **72**: 324–30. doi: [10.1043/0003-3219\(2002\)072<0324:COLCDI>2.0.CO;2](https://doi.org/10.1043/0003-3219(2002)072<0324:COLCDI>2.0.CO;2)
20. Dibbets JM, Nolte K. Effect of magnification on lateral cephalometric studies. *Am J Orthod Dentofacial Orthop* 2002; **122**: 196–201.
21. Bergersen EO. Enlargement and distortion in cephalometric radiography: compensation tables for linear measurements. *Angle Orthod* 1980; **50**: 230–44. doi: [10.1043/0003-3219\(1980\)050<0230:EADICR>2.0.CO;2](https://doi.org/10.1043/0003-3219(1980)050<0230:EADICR>2.0.CO;2)
22. Hassan B, van der Stelt P, Sanderink G. Accuracy of three-dimensional measurements obtained from cone beam computed tomography surface-rendered images for cephalometric analysis: influence of patient scanning position. *Eur J Orthod* 2009; **31**: 129–34.
23. Lee FCC, Noar JH, Evans RD. Evaluation of the CT scanogram for assessment of craniofacial morphology. *Angle Orthod* 2011; **81**: 17–25. doi: [10.2319/110809-630.1](https://doi.org/10.2319/110809-630.1)
24. Grauer D, Cevidanes LS, Proffit WR. Working with DICOM craniofacial images. *Am J Orthod Dentofacial Orthop* 2009; **136**: 460–70. doi: [10.1016/j.ajodo.2009.04.016](https://doi.org/10.1016/j.ajodo.2009.04.016)
25. Hassan B, Nijkamp P, Verheij H, Tairie J, Vink C, van der Stelt P, et al. Precision of identifying cephalometric landmarks with cone beam computed tomography *in vivo*. *Eur J Orthod* 2011; **35**: 38–44. doi: [10.1093/ejo/cjr050](https://doi.org/10.1093/ejo/cjr050)
26. Medelnik J, Hertrich K, Steinhäuser-Andresen S, Hirschfelder U, Hofmann E. Accuracy of anatomical landmark identification using different CBCT- and MSCT-based 3D images. [In German]. *J Orofac Orthop* 2011; **72**: 261–78.
27. Chang ZC, Hu FC, Lai E, Yao CC, Chen MH, Chen YJ. Landmark identification errors on cone-beam computed tomography-derived cephalograms and conventional digital cephalograms. *Am J Orthod Dentofacial Orthop* 2011; **140**: e289–97. doi: [10.1016/j.ajodo.2011.06.024](https://doi.org/10.1016/j.ajodo.2011.06.024)
28. Molen AD. Comparing cone beam computed tomography systems from an orthodontic perspective. *Semin Orthod* 2011; **17**: 34–8.

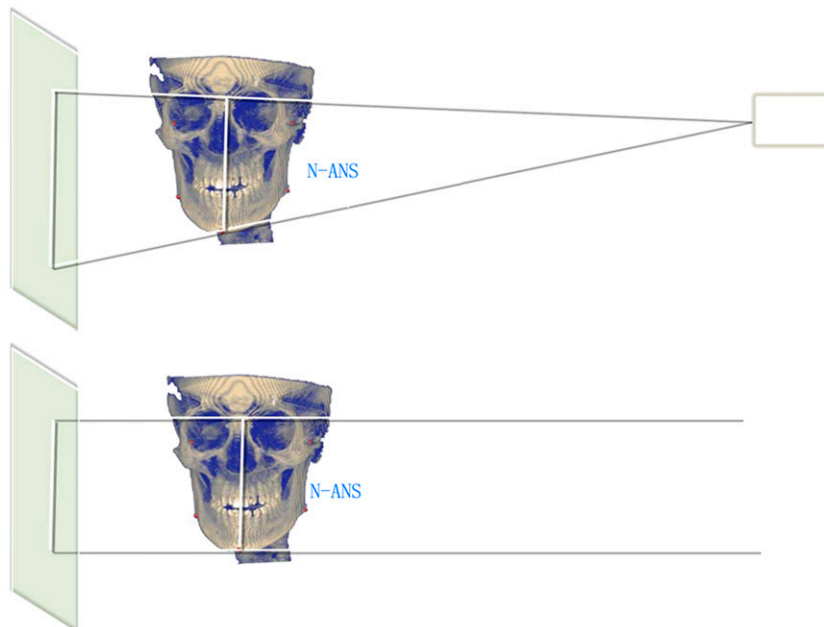


Figure 9 Illustration of distortion or enlargement of Type 1 on both cephalograms.

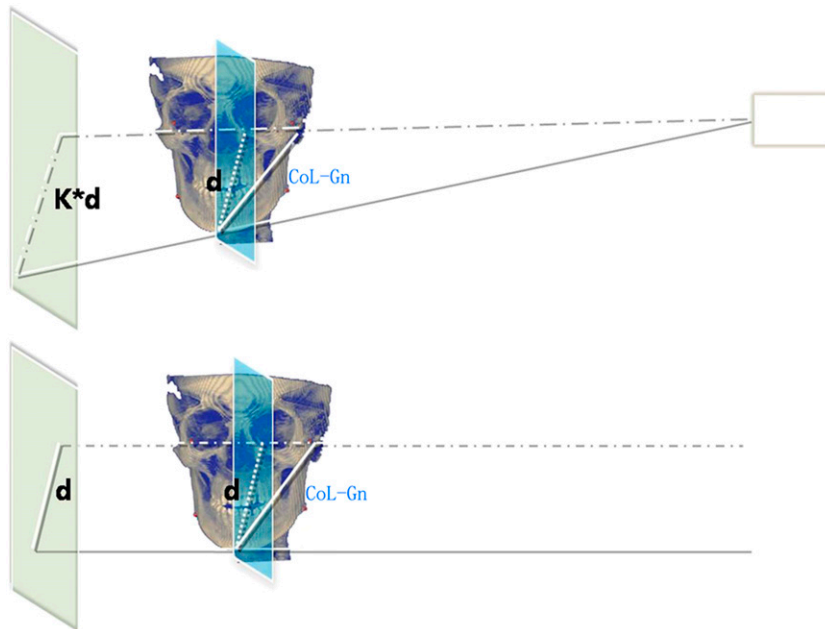


Figure 10 Illustration of distortion or enlargement of Type 2 on both cephalograms.

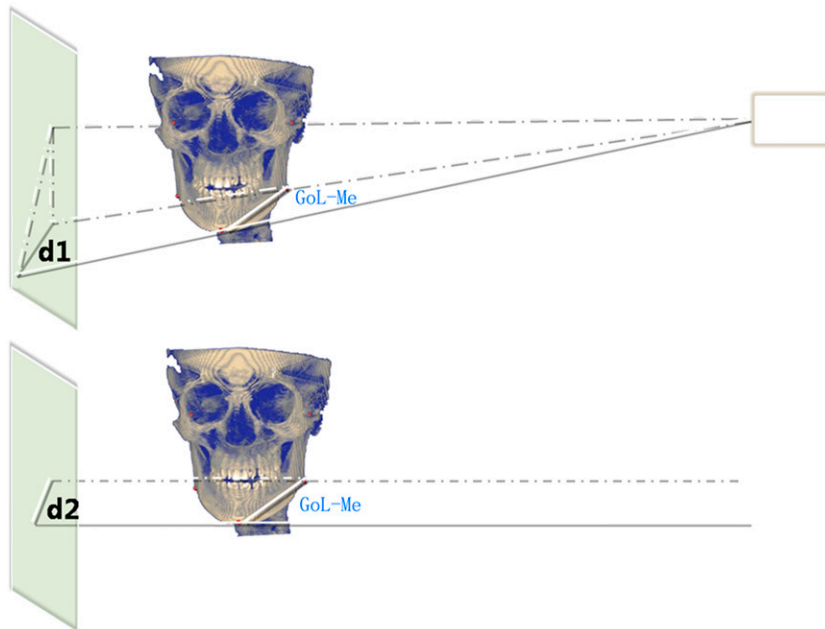


Figure 11 Illustration of distortion or enlargement of Type 3 on both cephalograms.